International Journal of Research in Engineering and Science (IJRES)
ISSN (Online): 2320-9364, ISSN (Print): 2320-9356
www.ijres.org Volume 10 Issue 3 ǁ 2022 ǁ PP. 14-19

Vector Distribution of Turbulent Parameters during Mass Transfer Process

Micheal Wilson[1*]
[*1]*University of North Florida, USA*

Abstract
Mass transfer occurrence is investigated in the current manuscript. At the beginning the geometry that is used for the simulation of the current study is explained and shown. The effect of turbulence behavior on mass transfer is investigated and explained.

Keywords: *Mass Transfer, Turbulence, Dissipation, Kinetic, Phase-Change*

Date of Submission: 05-03-2022 Date of acceptance: 21-03-2022

I. INTRODUCTION

Improving spray breakup and introducing smaller droplets within the combustion chamber is one of the most significant strategies for lowering exhaust emissions from compression ignition engines at the source. The spray formation is influenced by the flow inside the fuel injector nozzle. Cavitation happens when the local pressure falls below the liquid's vapor pressure at the same temperature [1-3]. The rapid flow of liquid through the tiny nozzle pores is accelerated by the substantial pressure drop across the injection nozzle [4-7]. As a result of the acceleration of the liquid inside the nozzle, there is a lot of turbulence, which causes the jet leaving the nozzle exit to be unstable [8, 9]. The streamlines are constricted at the sharp edges inside the nozzle holes, such as the entrance of the nozzle hole, reducing the effective cross section of the flow and causing the liquid to accelerate. According to the Bernoulli principle, this results in a decrease in local static pressure, which can drop to as low as the liquid's vapor pressure. The cavitation phenomenon causes cavitation bubbles to develop inside the nozzle bore. The cavitation bubbles are sucked into the combustion chamber from the nozzle [10]. When the bubbles are exposed to the pressure in the combustion chamber, they collapse and help to break up the spray even more [11-14]. This results in finer fuel droplets, which assists in quicker fuel evaporation. A critical environmental challenge is research into diesel injector systems for boosting combustion efficiency and fulfilling emission requirements from all sorts of diesel powertrains. To research and reduce soot emissions, several solutions have been proposed, including the use of diesel surrogates, additives in diesel and biodiesel mixes, multiple injections per power cycle, and increased injection pressure [15-19]. Upstream pressures in modern diesel engines are approximately 200 MPa, but the current tendency is to raise them to 300 MPa, as required by upcoming EU pollution rules. High injection pressures, on the other hand, will irreversibly generate very high fuel velocities, which, when combined with the rapid geometric changes in the injector passageways, will result in substantial pressure gradients and local depressurization [20]. The fuel may then vaporize if the pressure drops below the saturation threshold, a condition known as cavitation, which is linked to injector erosion and underperformance. High-pressure fuel injection systems are used in modern internal combustion engines [21-23]. When this high-pressure injection encounters an abrupt flow route shift, such as when approaching the nozzle region from the sac, the pressure lowers even further. These pressure dips can cause cavitation, which is predicted to have an effect on the external flow, such as changing the atomization process. Many recent investigations have focused on cavitation and atomization [21, 24-26]. Cavitation is the conversion of liquid to vapor when the local pressure falls below the saturation pressure and sufficient nucleation sites are present. Cavitation modeling has mostly been explored for pure fluids, or when a liquid species is surrounded by its own vapor species, such as cavitation in pure water. Cavitation may be simulated in a variety of ways in this scenario, and it is a hot field of research. On the one hand, two-phase models exist that simulate the liquid and vapor phases independently while taking into account the interaction between them. In cavitating systems, the placement of the interface is initially random. It is initially presumed that there are certain nucleation sites that will expand when the pressure decreases [27]. The beginning of cavitation and the development of cavitation bubbles are predicted using a mass transfer model. In diffused interface models, on the other hand, vapor and liquid are always treated as interpenetrating species, therefore there is no such thing as an exact crisp interface. One to a few thousand bubbles can be explored via scale resolving or direct numerical simulations (DNS). In actuality, millions of bubbles or even clouds of bubble clusters can exist. DNS of two-phase flows without phase change is considerably more restrictive than DNS of cavitation flows. To represent two-phase single fluid

cavitation, many modeling techniques have been studied. Parcels of cavitation bubbles are monitored using a Lagrangian formulation in Eulerian-Lagrangian models, while the main liquid flow field is calculated on an underlying Eulerian grid [28]. Each phase is solved with its own matching velocity field in the Euler-Euler (two-fluid) technique, but in the one-fluid Volume of Fluid (VOF) approach, the same velocity field is utilized for both phases [29]. Diffused-interface models (also known as continuum models or homogeneous mixture models) involve a mixture of vapor and liquid at the grid cell level and are driven by a specific Equation of State instead of tracking the interface (EOS). The thermal equilibrium hypothesis is commonly utilized in these models. This hypothesis assumes that phase transitions are endlessly quick and that the thermal equilibrium state is reached considerably faster than the time intervals relevant to the flow field [12]. Other formulations, such as momentum deficit or stochastic fields formulations, can also be used to simulate cavitating flows. Another technique to describe two-phase flow numerical simulations is to count how many equations must be solved to arrive at the final answer (terminology more commonly used for diffused interface or continuum type of models). These simulations are for any two-phase flow with phase change and/or many components in each phase [30]. The most complex technique in this nomenclature is the so-called seven equation model, which involves solving three equations for velocity, pressure, and temperature for each phase, as well as a single-phase transport equation to get the volume fraction of one of the phases. The five-equation model simplifies things even more. Each phase is in mechanical and thermal equilibrium in this model, and they share a common pressure and temperature field [31]. The four-equation model is a simplified version of the three-equation model, in which three equations for mixture mass, momentum, and energy are solved together with a partial density (or phase transport) equation with a sufficient mass transfer factor to allow for phase change. Because the process is assumed isothermal in many circumstances involving cavitation, the energy equation is often ignored, resulting in a three-equation model. Models with five and four equations offer a lot of possibilities for dealing with two-phase flows with phase change and phases with many components (e.g. when the gas phase consists of vapor and any other non-condensable gas). The primary challenge here is choosing the right EOS, which should be capable of handling both pure species and the transition or mixed area. The generic formulation to model two-phase flows with phase change that only included pure fluids (water and oxygen) with phase transformation between liquid and vapor was provided with a diffused interface and completely compressible system [32, 33]. The study advocated using a calibrated EOS, particularly the Noble-Able-Stiffened-Gas (NASF) EOS, that was tailored to a specified temperature range. The use of a diffused interface technique combined with a compressible formulation shown that such a formulation may replicate liquid cavitation in a multi-component gas system [34]. The vapor formed by the liquid plus any additional non-condensable gases present in the system make up the multi-component gas phase. The mass transfer rate was predicted using the difference in Gibbs energy between the liquid and vapor phases. The liquid phase in this scenario was always made up of a single species, and the effects of dissolved gas in the liquid were ignored [35]. It is well known that cubic equations of states may accurately predict the true fluid behavior of two-phase flows. In most circumstances, the above-mentioned continuum (diffuse interface) formulations are applicable for liquid jets that atomize but can cavitate during the acceleration phase inside the injector. The liquid-gas interface, on the other hand, is not implicitly considered in continuum models. Realistic scale resolving techniques for modeling atomization, on the other hand, have historically been based on interface resolving procedures, which presume a crisp contact between liquid and gas. It's still a difficult challenge to connect a diffuse interface strategy for internal cavitation to an interface re-solved approach. Methods utilizing both interface resolution and mixing techniques have been employed to mimic industrial scale problems including cavitation and atomization [36]. Liquid, vapor, and ambient gas (air) are thoroughly mixed at each cell level in a mixture-based formulation suggested before. For the liquid and vapor mixing, a barotropic equation of state is utilized, and the gas is assumed an isothermal ideal gas. The dispersed interface method restricts the prediction of atomization once more in this formulation. Due to the diffuse interface method's limitations, the formulation of the aforementioned phenomena takes into account surface density transfer to describe atomization and a homogeneous relaxation model to forecast vaporization [37, 38].

II. RESULT AND DISCUSSION

Figure 1 shows the geometry of the nozzle used for simulation in this study. The mentioned figure shows that the left and right reservoirs have equal dimensions to have symmetric behavior in the whole simulations. The middle narrow region is showing the orifice area in which cavitation phenomenon has a high potential to occur. The current geometry is derived from [39].

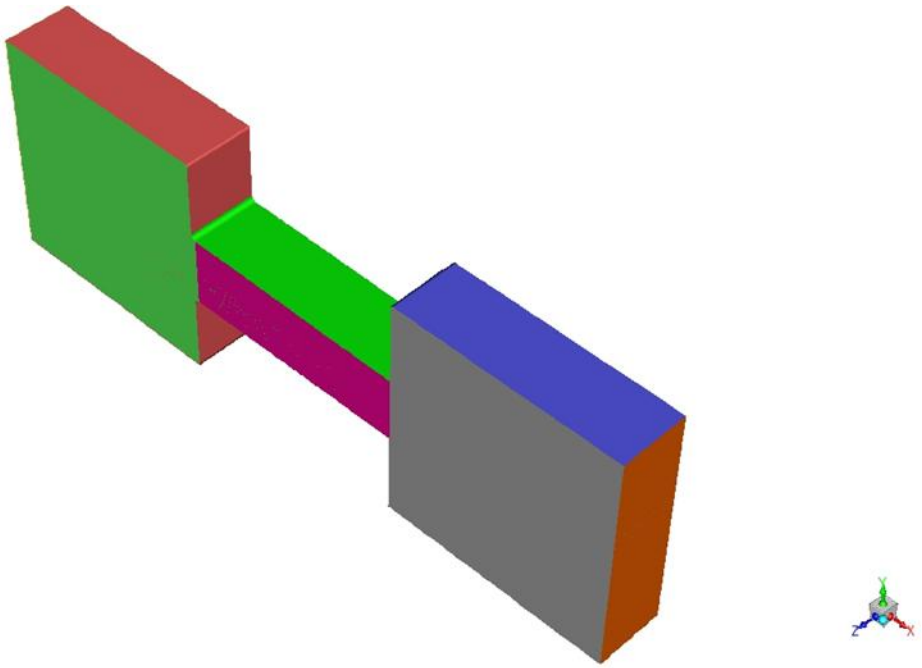

Figure 1: Geometry of the Wink nozzle used in this study.

Figure 2 shows distribution of the turbulent intensity along the nozzle geometry. In this figure the highest amount of turbulence occurs in the regions that mass transfer has high tendency of occurrence. Also, a high amount of turbulence intensity is visualized at the outlet of the orifice which is showing formation of spray phenomenon.

Figure 3 shows distribution of the turbulent kinetic energy as accumulation of numerous vectors. In this figure the highest amount of turbulent kinetic energy is seen mostly inside the orifice area which is due to mass transfer.
Figure 4 shows formation of dissipation in our simulation. In this figure the highest amount of dissipation is showing that a significant amount of energy is transferring and the only region that is showing the mentioned phenomenon is the regions that mass transfer occurs inside. The current results are comparable with what has been obtained earlier [40].

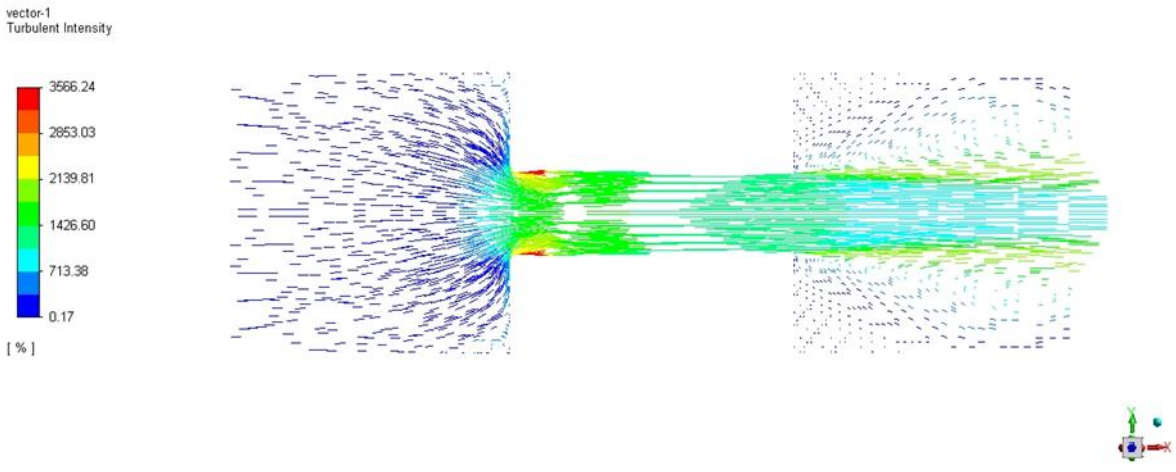

Figure 2: Turbulent intensity distribution shown as combination of vectors when cavitation starts.

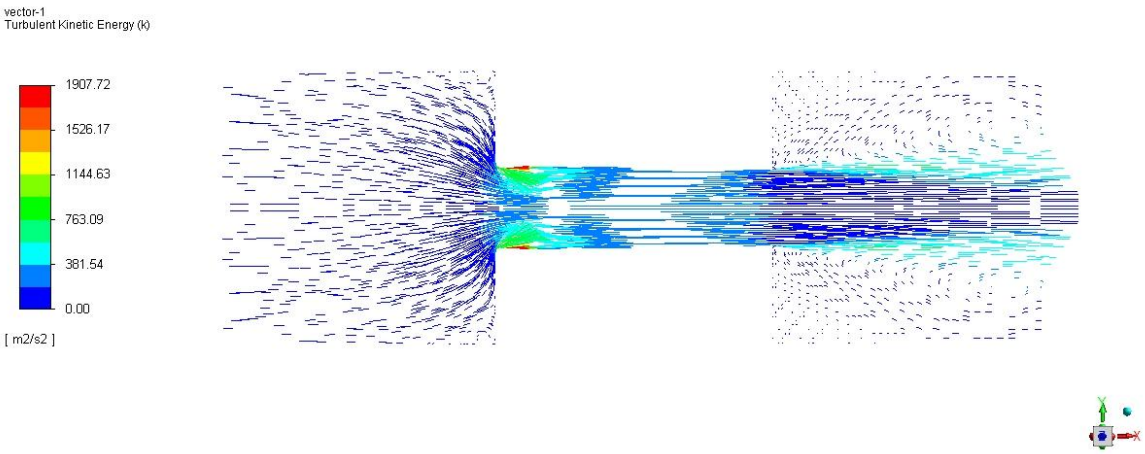

Figure 3: Turbulent Kinetic energy distribution shown as combination of vectors when cavitation starts.

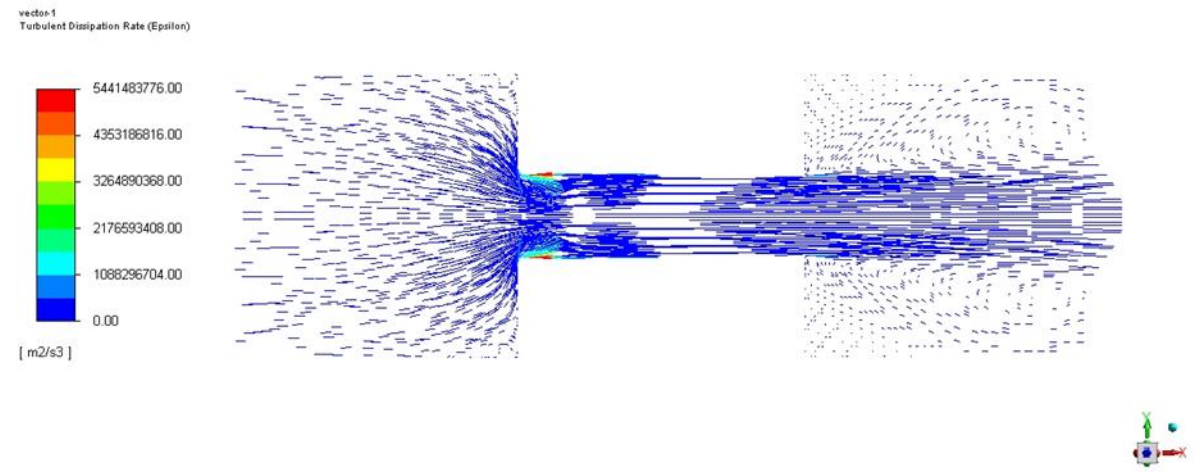

Figure 4: Turbulent dissipation rate distribution shown as combination of vectors when cavitation starts.
Figure 4: Strain rate distribution shown as combination of vectors when cavitation starts.

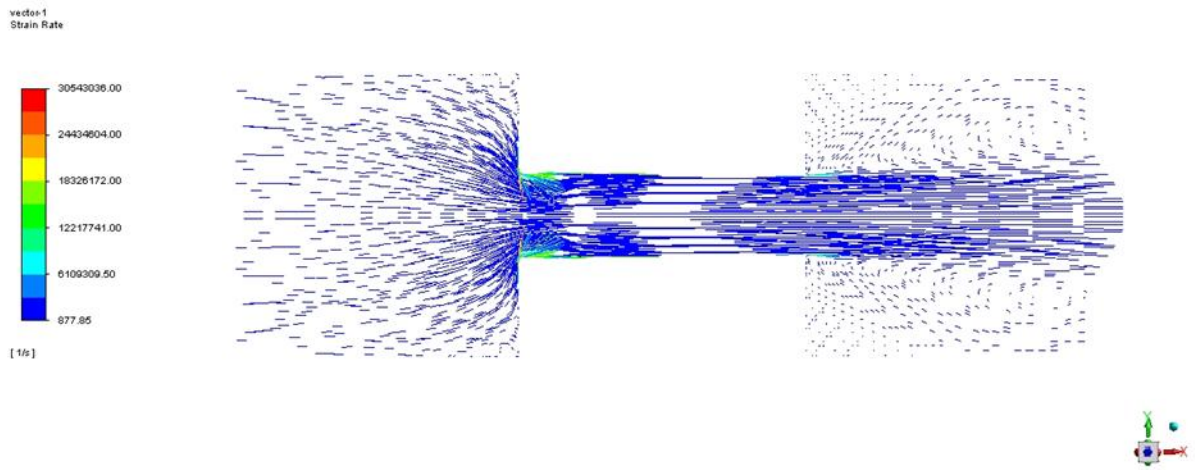

Figure 5: Strain rate distribution shown as combination of vectors when cavitation starts.

III. CONCLUSION

In the current study, using CFD method and finite volume method the flow inside a nozzle is investigated and the following conclusions has been made:

1) Turbulent dissipation rate increases significantly when mass transfer has tendency to occur.
2) Turbulent intensity also increases significantly in the orifice area.
3) Turbulent kinetic energy increases not only in the orifice area but also in the outlet reservoir.

REFERENCES

[1]. Reuter, F., et al., Wall Shear Rates Induced by a Single Cavitation Bubble Collapse, in Proceedings of the 10th International Symposium on Cavitation (CAV2018), J. Katz, Editor. 2018, ASME Press. p. 0.
[2]. Monakhov, A.A., I.L. Pankrat'eva, and V.A. Polyanskii, Vapor-Gas Cavitation and Accompanying Electrification in Sliding a Cylinder over a Surface. Fluid Dynamics, 2020. 55(3): p. 332-337.
[3]. Salvador, F.J., et al., Using a homogeneous equilibrium model for the study of the inner nozzle flow and cavitation pattern in convergent-divergent nozzles of diesel injectors. Journal of Computational and Applied Mathematics, 2017. 309: p. 630-641.
[4]. Zeng, S. and X.M. Du, Theoretical analysis and experimental research of non-cavitation noise on underwater counter-rotation propellers. Progress in Computational Fluid Dynamics, 2020. 20(1): p. 51-58.
[5]. Petkovsek, M., M. Hocevar, and P. Gregorcic, Surface functionalization by nanosecond-laser texturing for controlling hydrodynamic cavitation dynamics. Ultrasonics Sonochemistry, 2020. 67.
[6]. Pepperberg, I.M., Symbolic communication in the grey parrot, in The Oxford Handbook of Comparative Evolutionary Psychology, J. Vonk and T.K. Shackelford, Editors. 2012, Oxford University Press: New York. p. 297-319.
[7]. Hutli, E., M.S. Nedeljkovic, and S. Czifrus, STUDY AND ANALYSIS OF THE CAVITATING AND NON-CAVITATING JETS PART TWO Parameters Controlling the Jet Action and a New Formula for Cavitation Number Calculation. Thermal Science, 2020. 24(1): p. 407-419.
[8]. Ma, J.S., G.L. Chahine, and C.T. Hsiao, Spherical bubble dynamics in a bubbly medium using an Euler-Lagrange model. Chemical Engineering Science, 2015. 128: p. 64-81.
[9]. Holzhaider, J.C., et al., The social structure of New Caledonian crows. Animal Behaviour, 2011. 81(1): p. 83-92.
[10]. SMJ Zeidi, Miralam .Mahdi., Numerical investigation of the effect of different parameters on emitted shockwave from bubble collapse in a nozzle. Journal of Particle Science & Technology, 2021. 6(2): p. 13.
[11]. Farrell, K.J., Eulerian/Lagrangian analysis for the prediction of cavitation inception. Journal of Fluids Engineering-Transactions of the Asme, 2003. 125(1): p. 46-52.
[12]. Qiu, N., et al., Effects of microvortex generators on cavitation erosion by changing periodic shedding into new structures. Physics of Fluids, 2020. 32(10).
[13]. Abbasiasl, T., et al., Effect of intensified cavitation using poly(vinyl alcohol) microbubbles on spray atomization characteristics in microscale. Aip Advances, 2020. 10(2).
[14]. Wu, C.L., et al., Effect of cavitation jet processing on the physicochemical properties and structural characteristics of okara dietary fiber. Food Research International, 2020. 134.
[15]. Alagan, N.T., et al., Coolant boiling and cavitation wear - a new tool wear mechanism on WC tools in machining Alloy 718 with high-pressure coolant. Wear, 2020. 452.
[16]. Rasthofer, U., et al., Computational study of the collapse of a cloud with 12 500 gas bubbles in a liquid. Physical Review Fluids, 2019. 4(6): p. 063602.
[17]. Hong, F. and F. Zhang, Computational investigation of the cavitation vortex dynamics in flow over a three-dimensional hydrofoil by a new transport-based model. Proceedings of the Institution of Mechanical Engineers Part a-Journal of Power and Energy, 2020.

[18]. Stuppioni, U., et al., Computational Fluid Dynamics Modeling of Gaseous Cavitation in Lubricating Vane Pumps: An Approach Based on Dimensional Analysis. Journal of Fluids Engineering-Transactions of the Asme, 2020. 142(7).
[19]. Sezen, S. and S. Bal, Computational and Empirical Investigation of Propeller Tip Vortex Cavitation Noise. China Ocean Engineering, 2020. 34(2): p. 232-244.
[20]. Zeidi, S.M.J. and M. Mahdi, Evaluation of the physical forces exerted on a spherical bubble inside the nozzle in a cavitating flow with an Eulerian/Lagrangian approach. European Journal of Physics, 2015. 36(6).
[21]. Ge, M.Y., U. Svennberg, and R.E. Bensow, Investigation on RANS prediction of propeller induced pressure pulses and sheet-tip cavitation interactions in behind hull condition. Ocean Engineering, 2020. 209.
[22]. Chahine, G., Interaction between an oscillating bubble and a free surface. 1977.
[23]. Gevari, M.T., et al., Influence of Fluid Properties on Intensity of Hydrodynamic Cavitation and Deactivation of Salmonella typhimurium. Processes, 2020. 8(3).
[24]. Zeidi, S. and M. Mahdi, Investigation the effects of injection pressure and compressibility and nozzle entry in diesel injector nozzle's flow. Journal of Applied and Computational Mechanics, 2015. 1(2): p. 83-94.
[25]. Geng, L.L., J. Chen, and X. Escaler, Improvement of cavitation mass transfer modeling by including Rayleigh-Plesset equation second order term. European Journal of Mechanics B-Fluids, 2020. 84: p. 313-324.
[26]. Sagar, H.J., et al., Experimental and numerical investigation of damage on an aluminum surface by single-bubble cavitation. Materials Performance and Characterization, 2018. 7(5): p. 985-1003.
[27]. Aganin, A.A., et al., Evaluation of Thermal and Acoustic Energy during Collapse of Cavitation Bubbles. Journal of Machinery Manufacture and Reliability, 2020. 49(5): p. 367-373.
[28]. Asquier, N., J.Y. Chapelon, and C. Lafon, Evaluation of the Uncertainty of Passive Cavitation Measurements for Blood-Brain Barrier Disruption Monitoring. Ultrasound in Medicine and Biology, 2020. 46(10): p. 2736-2743.
[29]. Zhai, Z.M., T.R. Chen, and H.Y. Li, Evaluation of mass transport cavitation models for unsteady cavitating flows. Modern Physics Letters B, 2020. 34(2).
[30]. Horiba, T., T. Ogasawara, and H. Takahira, Cavitation inception pressure and bubble cloud formation due to the backscattering of high-intensity focused ultrasound from a laser-induced bubble. Journal of the Acoustical Society of America, 2020. 147(2): p. 1207-1217.
[31]. Chao, Q., et al., Cavitation intensity recognition for high-speed axial piston pumps using 1-D convolutional neural networks with multi-channel inputs of vibration signals. Alexandria Engineering Journal, 2020. 59(6): p. 4463-4473.
[32]. Chekh, O., et al., Cavitation in Nozzle: The Effect of Pressure on the Vapor Content. Advances in Design, Simulation and Manufacturing Ii, 2020: p. 522-530.
[33]. Koroteev, A.A., et al., Cavitation Effects on the Work of Disperse Sheet Collectors of Frameless Heat Removal Systems in Outer Space. Journal of Engineering Physics and Thermophysics, 2020. 93(6): p. 1311-1316.
[34]. Peng, H.N., et al., Cavitation bubble collapse between parallel rigid walls with the three-dimensional multi-relaxation time pseudopotential lattice Boltzmann method. Aip Advances, 2020. 10(10).
[35]. Joshi, S., et al., Bubble collapse induced cavitation erosion: Plastic strain and energy dissipation investigations. Journal of the Mechanics and Physics of Solids, 2020. 134.
[36]. Bai, L.X., et al., Cavitation in thin liquid layer: A review. Ultrasonics Sonochemistry, 2020. 66.
[37]. ikirica, A., et al., Cavitation Model Calibration Using Machine Learning Assisted Workflow. Mathematics, 2020. 8(12).
[38]. Soyama, H., Cavitation Peening: A Review. Metals, 2020. 10(2).
[39]. A Yazdi, M Nezamirad, S Amirahmadian, N Sabetpour, A Hamedi, Effect of Needle Height on Discharge Coefficient and Cavitation Number, International Journal of Aerospace and Mechanical Engineering 15 (7), 7.
[40]. A Yazdi, N Sabetpour, S Amirahmadian, M Nezamirad, A Hamedi, Effect of Pressure Difference and Needle Height on Formation of Cavitation in a real size nozzle, Fourth Conference on Technology Development in Mechanical and Aerospace Engineering, 2021.